Adaptive Suppression of High-Frequency Wide-Spectrum Vibrations with Application to Disk Drive Systems

Liting Sun, Xu Chen and Masayoshi Tomizuka

(CML Report)

Department of Mechanical Engineering
UC Berkeley

December 2014

Abstract

As the track density of HDDs increases, vibration suppression of the recording arm in HDDs is becoming more challenging. Vibrations in modern HDDs are environment/product-dependent with different frequency characteristics. Furthermore, they can occur at very high frequencies with wide spectral peaks, i.e, the energy of the vibrations concentrating at several frequency bands. In this report, an adaptive algorithm is presented to identify and suppress these high-frequency wide-spectrum vibrations. We design a vibration-compensation controller based on an adaptive disturbance observer (DOB), and devise parameter adaptation algorithms not only for the vibration frequencies but also for the spectral peak widths of the vibration. The peak-width parameters are adaptively tuned online to maximally attenuate the vibration with minimal error amplifications at other frequencies. The proposed algorithm is verified by simulations of HDDs for the problem of suppressing high-frequency wide-spectrum vibrations.

Contents

1 Introduction

According to a study by International Data Corporation (IDC)[16], the total amount of data in the world is now increasing exponentially and will reach 8ZB (2^{70} bytes) in 2015. The majority of the data needs to be stored in hard disk drive systems (HDDs), creating stringent requirements for larger storage capacity and faster data access speed in modern HDDs. However, as the track density increases, the control of the read/write head becomes more difficult. One of the greatest challenges comes from vibrations, which can occur in modern HDDs with their energy highly concentrated at several frequency bands and show up as spectral peaks with different widths. Both the center frequencies and the peak widths can change in different operation environments or within different HDD products. Furthermore, the spectral peaks can appear beyond the open loop servo bandwidth [6, 5]. These intrinsic characteristics make the high-frequency wide-spectrum vibrations difficult to suppress by traditional feedback controllers.

Various control algorithms have been developed for vibration suppression. Among them, disturbance observers (DOBs) [12] have attracted a great amount of attention due to their simplicity, light computational burden and good performance. For example, White et al. [17] augmented a feedback loop of a disk drive servo system with a DOB and realized $61\% - 96\%$ reduction of the vibrations at frequencies below 100Hz. Zheng and Tomizuka [18] suggested an adaptive disturbance observer which estimated the frequency of the disturbance and then canceled it. Jia et al. [8] also incorporated the adaptive frequency estimation into the traditional disturbance observer and achieved vibration rejection without losing the phase margin of the feedback system. Xu et al. [1, 3, 4] introduced a minimum-parameter adaptive Q filter in DOB and extended it to multiple-band cases, where disturbances with multiple width-limited spectral peaks can be accurately estimated and effectively rejected.

Most of previous studies have focused on the adaptation of the center frequencies with fixed width parameters [18, 1, 2, 9, 14, 3, 4]. In the cases of wide spectral peaks or time-varying spectral peak widths, however, it is hard to assure a good rejection performance under a fixed width parameter. If the selected width is too narrow, the spectral-peak vibrations cannot be effectively attenuated. If the selected width is too wide, the error amplifications at other frequencies caused by the "waterbed" effect will be large enough to cause strong degradation of control performance and may even destabilize

3

the system. Thus, adaptation of the peak width parameters is desired for effective disturbance attenuation with robustness and balanced overall performance. Results in this direction, however, are very limited in literature. Levin and Ioannou [10] proposed a controller with adaptive bandwidth using a multirate adaptive notch filter (ANF), but adaptation was only designed to estimate the system modal frequency and the tuning of the bandwidth was realized by multiple pre-designed controllers. This report proposes a controller based on a new adaptive DOB to suppress the above mentioned high-frequency wide-spectrum vibrations. In this new adaptive DOB, parameter adaptation algorithms are devised not only for the vibration frequencies but also for the spectral peak widths of the vibration so that maximal attenuation of the vibration can be achieved with minimal error amplifications at other frequencies. Another advantage of the proposed algorithm is that a lattice-form IIR (Infinite Impulse Response) notch filter [13] is incorporated into the Q-filter design in DOB, which offers more convenience and flexibility to adaptively tune the width parameters.

The remainder of the report is organized as follows. Section 2 describes the hard disk drive system and formulates the problem. The proposed DOB structure and new Q-filter design based on a lattice-form IIR notch filter are presented in Section 3. Section 4 gives the adaptation algorithm for the spectral peak width of the vibration. Section 5 verifies the effectiveness of the proposed algorithm through simulation results. Conclusions are given in Section 6.

2   Hard Disk Drive System

Notations throughout this report are as follows:

$P(z^{-1})$– HDD full-order plant
$P_n(z^{-1})$– HDD nominal model without delay
z^{-m}– delay in the HDD plant
$C(z^{-1})$– Baseline controller in HDD feedback loop
$Q(z^{-1})$– Q filter in DOB
$y(k)$– Output signal
$e(k)$– Position error signal (PES)
$u(k)$– Input control signal
$d(k)$– Disturbance signal
$n(k)$– Measurement noise

Bode Diagram
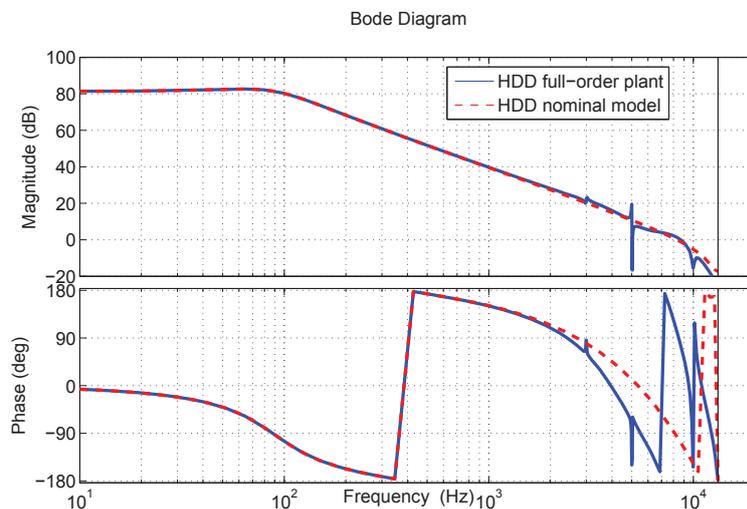
Figure 1: Frequency Response of the Full-Order Plant and Its Nominal Model

$\hat{d}(k)$– Estimate of the disturbance signal
$S_0(z^{-1})$– Baseline sensitivity function
$S(z^{-1})$– Sensitivity function of proposed control scheme

Figure 1 shows the frequency responses of the full-order HDD plant $P(z^{-1})$ and its low-order nominal model $z^{-m}P_n(z^{-1})$ provided by the open-source HDD simulation benchmark [7]. The sampling frequency F_s is $26,400$Hz. Several pre-designed notch filters[1] have been incorporated into $P(z^{-1})$ for attenuation of the high-frequency resonances. Additionally, the frequency response in Fig. 1 shows that the nominal model accurately matches the actual dynamics of the plant up to about 2kHz.

The baseline sensitivity function $S_0(z^{-1})$ obtained by a PID controller $C(z^{-1})$ is shown in Fig. 2. Note that above the servo bandwidth, the system has limited performance for disturbance rejection and a wide error amplification region due to the "waterbed" effect. If the high-frequency wide-spectrum excitations enter the HDDs with their spectral peaks above the

---

[1]These Notch filters are designed to cancel the physical resonances of the plant. Four second-order notch filters are incorporated, with notches centered at 4.1kHz, 5.0kHz, 8.2kHz and 12.3kHz. Note that the center frequencies of the notches introduced here differ from the one addressed in Section 3.

servo bandwidth, the vibrations will be greatly amplified and degrade the track-following performance. Moreover, limited by the "waterbed" effect, more considerations must be given at those frequencies to "locally" shape the sensitivity function for enhanced vibration suppression. Neither a too narrow nor a too wide attenuation range will achieve good performance. Also, when the vibration spectral peak widths change, the control parameters should be adaptively tuned to maintain the performance.
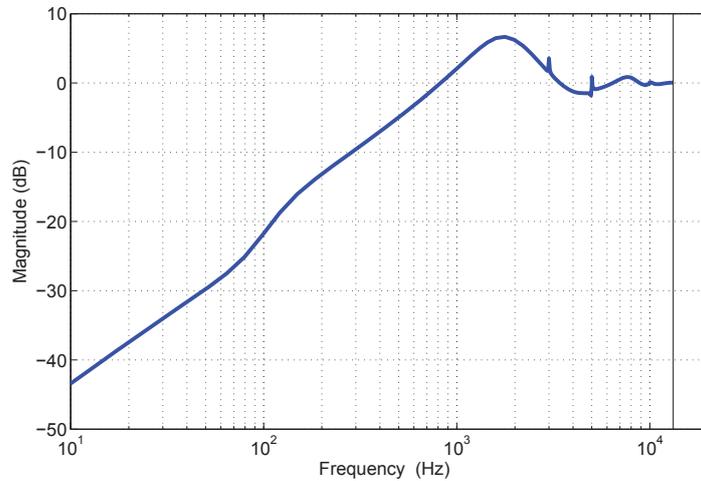
Figure 2: Frequency Response of the Baseline Sensitivity Function

3 DOB Structure with New Lattice-Form Notch Filter in Q Filter Design

3.1 DOB Structure for Vibration Suppression

The proposed DOB structure for vibration suppression is shown in Fig.3. We assume that all excitations enter the HDDs as a lumped disturbance $d(k)$. The estimate of the disturbance, $\hat{d}(k)$, is constructed as:

$$
\begin{aligned}
\hat{d}(k) &= P_n^{-1}(q^{-1}) \left[P(q^{-1}) \left(d(k) + u(k) \right) + n(k) \right] - q^{-m} u(k) \\
&= P_n^{-1}(q^{-1}) P(q^{-1}) d(k) + \left[P_n^{-1}(q^{-1}) P(q^{-1}) - q^{-m} \right] u(k) \\
&\quad + P_n^{-1}(q^{-1}) n(k),
\end{aligned} \tag{1}
$$

6
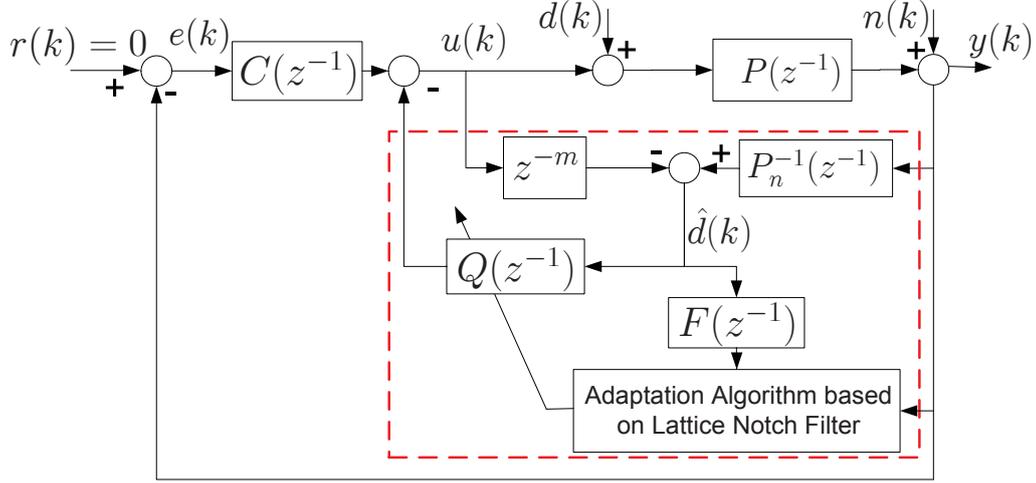
Figure 3: The Proposed DOB Structure for Vibration Suppression

where q^{-1} denotes the one-step delay operation in time domain. It can then be derived that the transfer function from $d(k)$ to $e(k)$ is

$$G_{d2e}(z^{-1}) = \frac{-(1 - z^{-m}Q(z^{-1}))P(z^{-1})}{1 + P(z^{-1})C(z^{-1}) + Q(z^{-1})\left(P(z^{-1})P_n^{-1}(z^{-1}) - z^{-m}\right)} \qquad (2)$$

Notice that an accurate model is available at frequencies below 2kHz (see Fig. 1), i.e., $z^{-m}P_n(z^{-1}) \approx P(z^{-1})$ below 2kHz. Applying this approximation, Eqs. (1) and (2) can be simplified as:

$$\hat{d}(k) \approx q^{-m}d(k) + P_n^{-1}(q^{-1})n(k) \qquad (3)$$

$$G_{d2e}(z^{-1}) \approx -\frac{P(z^{-1})(1 - z^{-m}Q(z^{-1}))}{1 + P(z^{-1})C(z^{-1})} \qquad (4)$$

Note that the factor $1/[1 + P(z^{-1})C(z^{-1})]$ in Eq. (4) is the baseline sensitivity function $S_0(z^{-1})$ and referring Fig. 3, $G_{d2e}(z^{-1})$ is equal to the closed-loop sensitivity function $S(z^{-1})$ multiplied by $-P(z^{-1})$. Thus, we can express $S(z^{-1})$ as:

$$S(z^{-1}) \approx \left(1 - z^{-m}Q(z^{-1})\right)S_0(z^{-1}) \qquad (5)$$

i.e., the closed-loop sensitivity function $S(z^{-1})$ is approximately the product between the baseline sensitivity function $S_0(z^{-1})$ and an add-on model-free

7

factor $1 - z^{-m}Q(z^{-1})$. This approximation transforms the shaping of the sensitivity function into the design of a proper Q filter and introduces more design flexibility.

When model uncertainty exists, $P(z^{-1})$ can be expressed as:

$$P(z^{-1}) = z^{-m}P_n(z^{-1})(1 + \triangle(z^{-1})) \tag{6}$$

where $\triangle(z^{-1})$ represents the multiplicative uncertainty term. Then $G_{d2e}(z^{-1})$ in Eq. (2) becomes

$$G_{d2e}(z^{-1}) = \frac{P(z^{-1})(z^{-m}Q(z^{-1}) - 1)}{1 + P(z^{-1})C(z^{-1}) + Q(z^{-1})z^{-m} \triangle (z^{-1})} \tag{7}$$

A sufficient condition to guarantee the robust stability of the closed-loop system is: $|Q(z^{-1})z^{-m} \triangle (z^{-1})| < |1 + P(z^{-1})C(z^{-1})|$, i.e.,

$$|Q(e^{-j\omega})| < \left| \frac{1}{S_0(e^{-j\omega}) \triangle (e^{-j\omega})} \right|, \forall \omega. \tag{8}$$

3.2 Q-filter Design based on Lattice-form IIR Notch Filters

Based on Eq. (5), the design of the Q filter in this DOB structure is of great importance for vibration suppression. Recall from Eq. (3) that $\hat{d}(k)$ is a contaminated and m-step delayed disturbance estimate. Therefore, in order to effectively compensate and cancel the wide-band disturbance, the Q filter should be a band-pass filter whose passband is located at the spectral peak of the disturbance. With a well tuned passband in Q, the major frequency components of the disturbance will be filtered out and fed back into the control signal for cancellation. Therefore, within frequency ranges where $z^{-m}P_n(z^{-1}) \approx P(z^{-1})$ is satisfied and the measurement noise $n(k)$ is small compared to the disturbance contribution, the steady state PES $e(k)$ will be given by:

$$
\begin{aligned}
e(k) &= -\left(1 - q^{-m}Q(q^{-1})\right) S_0(q^{-1})P(q^{-1})d(k) \qquad (9) \\
&= -S_0(q^{-1}) \left(\frac{A_Q(q^{-1}) - q^{-m}B_Q(q^{-1})}{A_Q(q^{-1})} \right) P(q^{-1})d(k)
\end{aligned}
$$

where $B_Q(q^{-1})$ and $A_Q(q^{-1})$ are the numerator and denominator of the Q filter, respectively.

Assume that $d(k)$ contains only one spectral peak centered at f_0 (in Hz), i.e., the major component of $d(k)$ can be approximately constructed as a sinusoidal signal with frequency at f_0 (in Hz). Based on Internal Mode Principle (IMP), we have $(1 - 2\cos\omega_0 z^{-1} + z^{-2})sin(\omega_0 k + \phi) = 0$, where $\omega_0 = 2\pi f_0 T_s$. Therefore, for a small steady state $e(k)$ in the presence of $d(k)$, $1 - z^{-m}Q(z^{-1})$ in Eq. (9) should contain an IMP-based notch filter $N(z^{-1})$, whose notch width (NW, the difference between the upper and lower frequencies where the notch filter gains are -3dB) can be adaptively tuned to cover the spectral peak of $d(k)$. Here, we choose the denominator of $Q(z^{-1})to$ be equal to that of $N(z^{-1})$, i.e., $A_Q(z^{-1}) = A_N(z^{-1})$, as shown in Eqs. (10) - (12). $J(z^{-1})$ in Eq. (10) is a FIR (Finite Impulse Response) polynomial of z^{-1}.

$$1 - z^{-m}Q(z^{-1}) = N(z^{-1})J(z^{-1}) \tag{10}$$

$$\frac{A_Q(z^{-1}) - z^{-m}B_Q(z^{-1})}{A_N(z^{-1})} = \frac{B_N(z^{-1})}{A_N(z^{-1})}J(z^{-1}) \tag{11}$$

$$1 - 2\cos\omega_0 z^{-1} + z^{-2} = B_N(z^{-1}) \tag{12}$$

With this choice, Eq. (11) can be written as:

$$A_N(z^{-1}) = z^{-m}B_Q(z^{-1}) + B_N(z^{-1})J(z^{-1}) \tag{13}$$

Equation (13) is a Diophantine Equation (DE) where we can solve for $B_Q(z^{-1})$ and $J(z^{-1})$ once a proper notch filter $N(z^{-1})$ is designed.

Now we have transformed the shaping of $S(z^{-1})$ into the design of a proper notch filter with desired notch width at the center frequency of the vibration spectral peak, f_0. As for the structure of notch filters, previous research on ANF or adaptive DOB has studied the usage of direct-form notch filters. Transfer function of the direct-form notch filter is given in Eq. (14), where ω_0 determines the center frequency of the notch and $\alpha \in [0, 1]$ controls the notch width, as defined in Eq. (15). The smaller the parameter α, the wider the notch width (NW).

$$N(z^{-1}) = \frac{1 - 2\cos\omega_0 z^{-1} + z^{-2}}{1 - 2\alpha\cos\omega_0 z^{-1} + \alpha^2 z^{-2}} \tag{14}$$

$$NW \approx \pi(1 - \alpha) \tag{15}$$

As mentioned in Section 1, wide-band vibrations are environment- or product-dependent. Both the center frequency of the spectral peak and
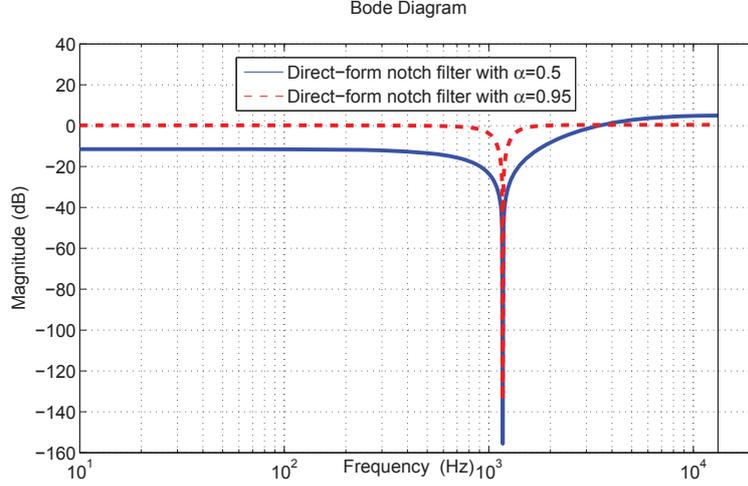
Figure 4: Frequency Response of Direct-Form Notch Filters with Different Notch Widths

the peak width can change in different situations. Adaptation to both the frequency parameter $\cos \omega_0$ and width parameter α is desired for better vibration-suppression performance. The nonlinearity with respect to α in Eq. (14), however, makes the width adaptation quite difficult to implement. Also, the frequency response of direct-form notch filter $N(z^{-1})$ in Eq. (14) is not symmetric at low and high frequencies, as shown in Fig. 4. The wider the notch, the more amplifications at high frequencies. Therefore, although $N(z^{-1})$ provides enhanced low gain near the notch center and at low frequencies, the high frequency gain should be carefully handled for wide-band designs to avoid undesired noise/disturbance amplifications.

To solve these problems, a new lattice-form notch filter, denoted by $N_L(z^{-1})$, is introduced in the proposed wide-spectrum vibration suppression algorithm. The transfer function of $N_L(z^{-1})$ and its frequency responses with different notch widths are shown in Eq. (16) and Fig. 4. Similarly, ω_0 determines the center frequency of the notch and α_L controls the notch

10

width.

$$N_L(z^{-1}) = \frac{1 - 2\cos\omega_0 z^{-1} + z^{-2}}{1 - (1 + \alpha_L)\cos\omega_0 z^{-1} + \alpha_L z^{-2}} \quad (16)$$

$$NW = 2\arctan\frac{1 - \alpha_L}{1 + \alpha_L} \quad (17)$$

Equation (16) indicates that, compared to the direct-form notch filter $N(z^{-1})$ in Eq. (14), $N_L(z^{-1})$ is bilinear with respect to both the frequency parameter $\cos\omega_0$ and the width parameter α_L. This bilinearity makes the design amenable to adaptation of both the notch-width parameter and the center-frequency parameter. Additionally, Fig. 5 shows that lattice notch filters have symmetric gains at low and high frequencies, regardless of the notch location and width.
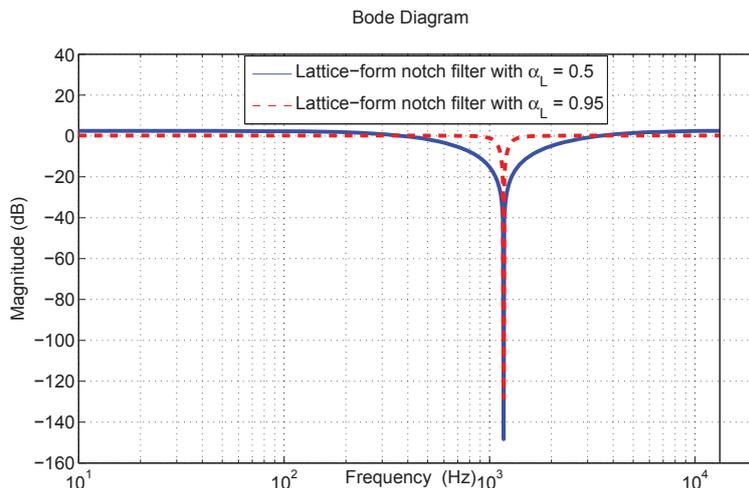
Figure 5: Frequency Response of Lattice-Form Notch Filters with Different Notch Widths

Combining Eqs. (11), (13) and (16), we can construct a Q filter with adaptive passband frequency and passband width in DOB to maximally attenuate the various wide-spectrum vibrations. For example, if the system has one-step delay, i.e., $m = 1$, then the corresponding Q filter (the center frequency is set to 1172Hz) is given by

$$Q(z^{-1}) = \frac{(1 - \alpha_L)\cos\omega_0 + (\alpha_L - 1)z^{-1}}{1 - (1 + \alpha_L)\cos\omega_0 z^{-1} + \alpha_L z^{-2}}. \quad (18)$$

Figure 6 shows the frequency response of Eq. (18), where the band-pass property is evident.
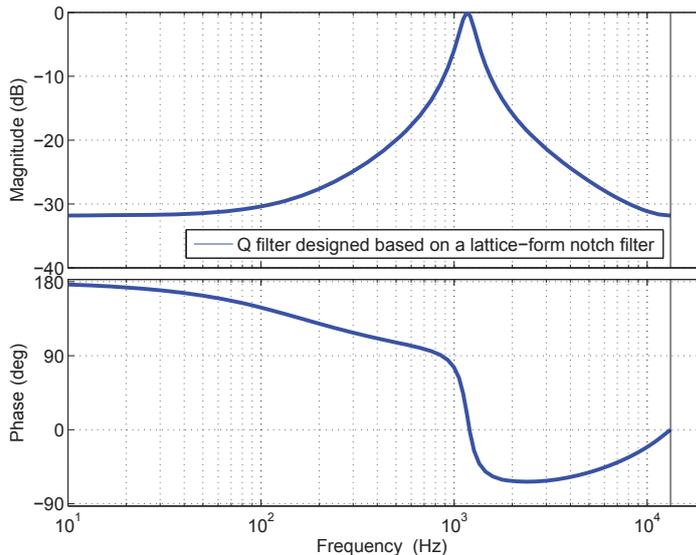
Figure 6: Frequency Response of the Q Filter Designed Based on Lattice-Form Notch Filter ($m = 1$)

4   Peak-Width Adaptation Algorithm

Recalling Eqs. (9), (10) and (11), we aim at designing an adaptive Q filter to minimize the PES signal $e(k)$ in the presence of wide-spectrum vibrating excitations $d(k)$. The design of Q filter requires knowledge of the frequency information $\beta = \cos \omega_0$ and the width parameter α_L, which are not available in advance. As a number of previous studies have addressed the frequency identification methods explicitly, here we focus on the adaptation of α_L and assume that β is known. Notice that, in order to suppress the wide-band vibrations, the notch width of $N_L(z^{-1})$ should be wide enough to cover the spectral peak of the vibrations, but not too wide to become a non-notch filter[2] which brings intolerant amplifications at other frequencies due to the

---

[2]As the notch becomes wider, the depth of the notch becomes shallower.

"waterbed" effect. A nice balance between the vibration suppression and the error amplifications should be found adaptively.

Equation (9) suggests that minimizing $e(k)$ without changing $S_0(z^{-1})$ is equivalent to minimizing $(1-q^{-m}Q(q^{-1}))e_b(k)$, where $e_b(k) = P(q^{-1})S_0(q^{-1})d(k)$ reflects the baseline PES. $\hat{d}(k)$, as a m-step delayed and contaminated estimate of $d(k)$ (Eq. (3)), has spectral characteristics which are similar to $d(k)$ (when $n(k)$ is small). In Fig. 3, let $F(z^{-1}) = P_n(z^{-1})/(1 + P_n(z^{-1})C(z^{-1}))$ and $c(k) = F(q^{-1})\hat{d}(k)$, where $F(z^{-1})$ is a nominal version of $P(z^{-1})S_0(z^{-1})$. Then the spectral characteristics of $e_b(k)$ will be preserved in $c(k)$. Therefore, the best notch width α_L^o can be obtained by minimizing the following cost function:

$$V_k = \sum_{j=1}^{k} \frac{1}{2}\lambda^{k-j}(k)[e_L^0(j)]^2 \tag{19}$$

where $\lambda(k)$ is a time-varying forgetting factor[3] and $e_L^0(j)$ is the *a priori* estimation error, obtained by passing $c(k)$ through an adaptive lattice-form IIR notch filter $N_L(z^{-1})$, i.e.,

$$
\begin{aligned}
e_L^0(k) &= N_L(q^{-1})c(k) \\
&= \frac{1 - 2\beta q^{-1} + q^{-2}}{1 - (1 + \hat{\alpha}_L(k-1))\beta q^{-1} + \hat{\alpha}_L(k-1)q^{-2}}c(k),
\end{aligned}
$$

which is equivalent to

$$
\begin{aligned}
e_L^0(k) &= \beta(1 + \hat{\alpha}_L(k-1))e_L^0(k-1) - \hat{\alpha}_L(k-1)e_L^0(k-2) \\
&\quad + c(k) - 2\beta c(k-1) + c(k-2). \tag{20}
\end{aligned}
$$

For the related adaptation algorithm, we apply the Recursive Prediction-Error Method (RPEM) which guarantees unbiased local convergence. The recursive adaptation algorithm is expressed as follows:

$$F(k) = \frac{1}{\lambda(k)}\left\{F(k-1) - \frac{F(k-1)\phi(k-1)\phi^T(k-1)F(k-1)}{\lambda(k) + \phi^T(k-1)F(k-1)\phi(k-1)}\right\} \tag{21}$$

$$\hat{\alpha}_L(k) = \hat{\alpha}_L(k-1) + F(k-1)\phi(k-1)e_L^0(k) \tag{22}$$

---

[3]One common design is to exponentially change λ from its initial value $\lambda(0)$ to λ_{end}, with a convergence speed defined by λ_{rate}, i.e., $\lambda(k) = \lambda_{end} - (\lambda_{end} - \lambda(k))\lambda_{rate} \in (0, 1)$

where $\phi(k-1)$ is the negative of the gradient of $e_L^0(k)$ with respect to the latest estimated parameter $\hat{\alpha}_L(k-1)$, defined by $\phi(k-1) = -\partial e_L^0(k)/\partial\hat{\alpha}_L(k-1)$.

To obtain $\phi(k-1)$, we notice the following relationship,

$$
\begin{aligned}
\phi(k-1) & = -\frac{\partial e_L^0(k)}{\partial\hat{\alpha}_L(k-1)} \\
& = -\frac{\partial N_L(\hat{\alpha}_L(k-1), q^{-1})}{\partial\hat{\alpha}_L(k-1)}c(k) \\
& = -\frac{\partial N_L(\hat{\alpha}_L(k-1), q^{-1})}{\partial\hat{\alpha}_L(k-1)}N_L^{-1}(\hat{\alpha}_L(k-1), q^{-1})e_L^0(k) \\
& = -\frac{q^{-1}(q^{-1}-\beta)}{1-(1+\hat{\alpha}_L(k-1))\beta q^{-1}+\hat{\alpha}_L(k-1)q^{-2}}e_L^0(k)
\end{aligned}
\tag{23}
$$

So $\phi(k-1)$ can be recursively expressed as follows:

$$
\begin{aligned}
\phi(k-1) & = \beta\left[1+\hat{\alpha}_L(k-1)\right]\phi(k-2) - \hat{\alpha}_L(k-1)\phi(k-3) \\
& \quad +\beta e_L^0(k-1) - e_L^0(k-2)
\end{aligned}
\tag{24}
$$

To improve the estimation precision and increase the convergence rate, the *a posteriori* error $\bar{e}_L(k)$ is introduced to update Eq. (20) and Eq. (24) [11]. The adaptation algorithm can then be summarized as follows:

Initialization: $\hat{\alpha}(0) = 0.5$; $F(0) = 100/E[e_L^0(0)]^2$; $\phi(0) = \phi(-1) = 0$; $\bar{e}_L(-1) = \bar{e}_L(-2) = 0$.

Main loop: for $k = 1, 2, ...$

$$
\begin{aligned}
e_L^0(k) & = \beta(1+\hat{\alpha}_L(k-1))\bar{e}_L(k-1) - \hat{\alpha}_L(k-1)\bar{e}_L(k-2) \\
& \quad +c(k) - 2\beta c(k-1) + c(k-2)
\end{aligned}
\tag{25}
$$

$$
\hat{\alpha}_L(k) = \hat{\alpha}_L(k-1) + F(k-1)\phi(k-1)e_L^0(k)
\tag{26}
$$

$$
F(k) = \frac{1}{\lambda(k)}\left\{F(k-1) - \frac{F(k-1)\phi(k-1)\phi^T(k-1)F(k-1)}{\lambda(k) + \phi^T(k-1)F(k-1)\phi(k-1)}\right\}
\tag{27}
$$

$$
\begin{aligned}
\bar{e}_L(k) & = \beta(1+\hat{\alpha}_L(k))\bar{e}_L(k-1) - \hat{\alpha}_L(k)\bar{e}_L(k-2) \\
& \quad +c(k) - 2\beta c(k-1) + c(k-2)
\end{aligned}
\tag{28}
$$

$$
\begin{aligned}
\phi(k) & = \beta\left[1+\hat{\alpha}_L(k)\right]\phi(k-1) - \hat{\alpha}_L(k)\phi(k-2) \\
& \quad +\beta\bar{e}_L(k) - \bar{e}_L(k-1)
\end{aligned}
\tag{29}
$$

REMARK 1: If no prior knowledge of the center frequency parameter β is available, adaptation will be divided into two stages due to the nonlinear product term of β and α_L in $N_L(z^{-1})$. In the first stage, β is estimated with a fixed notch width using ANF techniques. At this stage, α_L can be set to be close to 1 for more accurate frequency estimation. Then with the estimated β, adaptation will be switched to α_L using the proposed algorithm.

REMARK 2: Due to the local-minima convergence of RPEM, initial values of α_L will influence the performance. To enhance convergence, low and high bounds for α_L should be introduced during the adaptation.

5   Case Study and Simulation Results

The proposed algorithm was implemented in the HDD simulation benchmark [7]. The delay in the augmented plant $P(z^{-1})$ is $m = 3$, with a sampling time of $T_s = 3.7878 \times 10^{-5}$sec. A set of vibration excitations generated from actual HDD measurements with wide high-frequency spectral peaks are used for algorithm verification.

Figure 7 and Fig. 8 show the spectra of the vibration signal and the corresponding baseline PES signal. Recalling the baseline controller in Fig. 3 and the baseline sensitivity function in Fig. 2, we can see clearly that the first spectral peak centered at around 100Hz has been significantly attenuated by the baseline controller, but the second peak at 1172Hz is greatly amplified, resulting in a larger PES in HDDs.
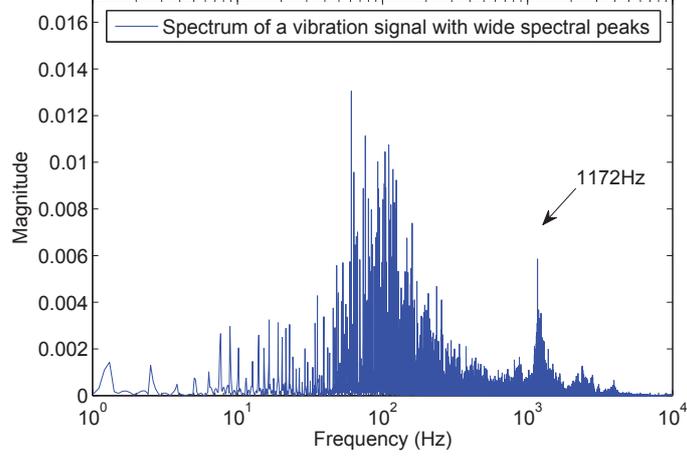
Figure 7: Spectrum of a Vibration Signal with Wide Spectral Peaks
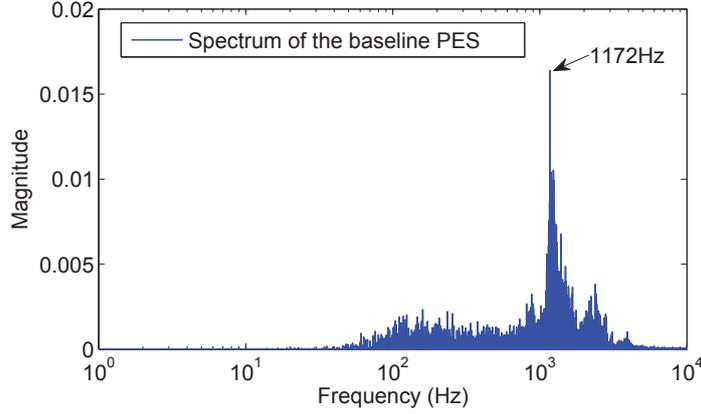
Figure 8: Spectrum of the Baseline PES Signal in the Presence of Vibration Signal in Figure7

Figure 9 illustrates the relationship between the passband width parameter α_L and the vibration-suppression performance in terms of a 3σ value of the PES signal. In this group of simulations, different values are selected for the width paramter α_L with a same frequency parameter set as $\beta = \cos(2\pi f_0 T_s)(f_0 = 1172\text{Hz})$, so that the Q filter in the DOB has different passband widths with fixed central frequency at 1172Hz. Figure 9 indicates that: 1) with the proposed DOB compensator as shown in Fig. 3 (within

16

the dashed box), vibrations will be greatly suppressed; 2) there exists an optimal value for the width parameter α_L ($\alpha_L^{opt} = 0.83$ in this case study) for minimization of the 3σ value of the PES signal. With α_L^{opt}, the spectral peak of the vibration at $f_0 = 1172$Hz can be maximally suppressed with minimal influences at other frequencies.
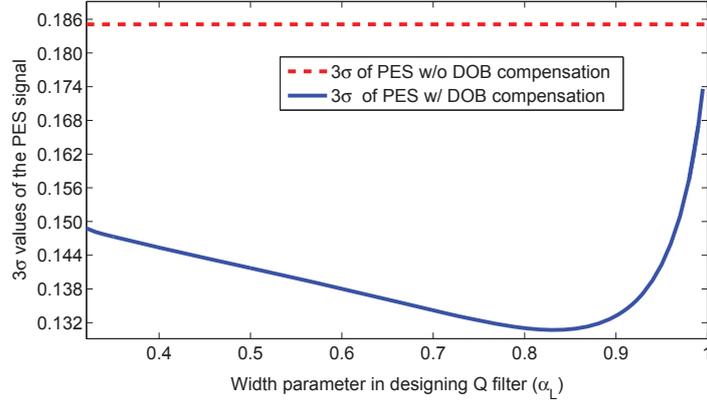
Figure 9: Relationship Between the Peak Width Parameter α_L and the Performance of the DOB Compensator
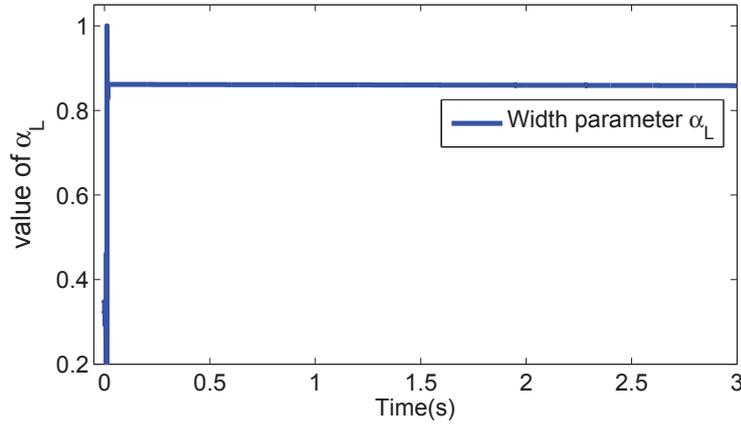
Figure 10: The Convergence of the Passband Width Parameter α_L

The proposed passband-adaptive DOB is then implemented to suppress

the same vibration shown in Fig.7. The adaptation of the passband width parameter α_L in Q filter is shown in Fig. 10, where the converged value is $\alpha_L^{opt} = 0.86$, very close to the manually tuned optimal value in Fig. 9. The bias is due to the local convergence of the RPEM algorithm. However, as shown in Fig.9, the converged value of α_L in the proposed algorithm is within the suboptimal set so that sufficient suppression to the vibrations will be provided.

Time trace and spectrum of the PES obtained by the proposed adaptive algorithm are shown in Fig.11 and Fig.12, respectively. It can be seen that the 3σ value of the PES has been reduced from 18.57% to 13.25%. The spectral peak at 1172Hz has been effectively attenuated without causing large amplifications at other frequencies. The resulting new sensitivity function in Fig.13 also shows a significant performance enhancement at around 1172Hz, although the performance at low frequencies has been slightly sacrificed due to the "waterbed" effect.
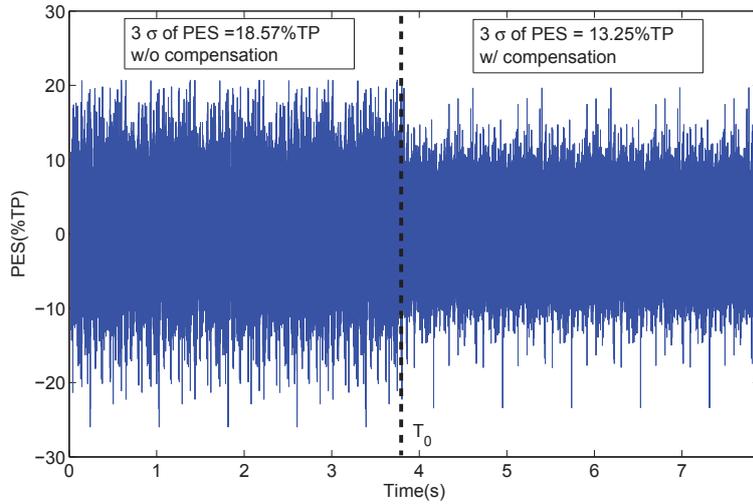
Figure 11: PES Time Traces with and without Passband-adaptive DOB

18
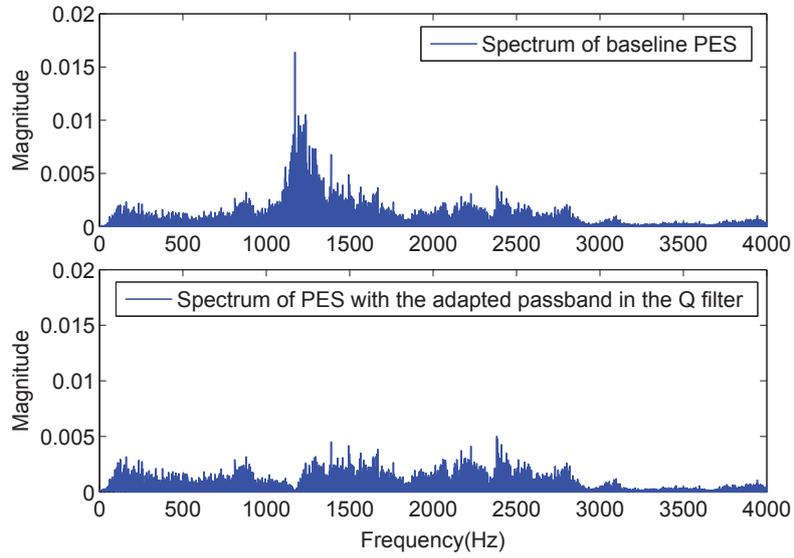
Figure 12: Spectrum of the PES Signals without and with Proposed Passband-Adaptive DOB
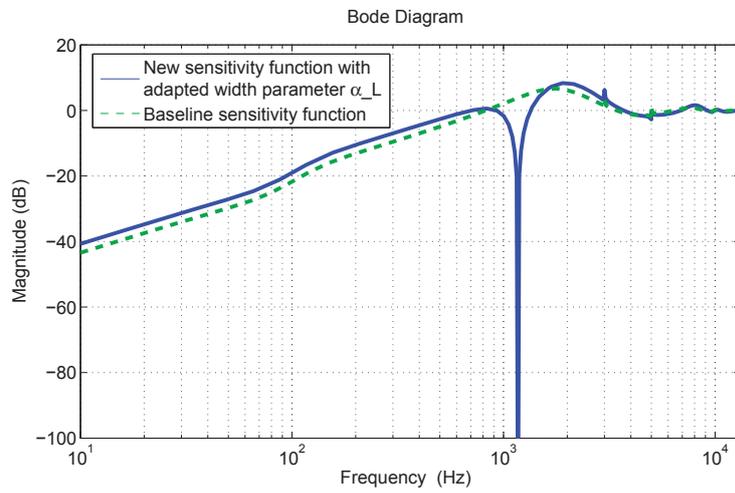
Figure 13: The Baseline Sensitivity Function and the new Sensitivity Function with Passband-Width Adaptive DOB

6   Conclusion

In this report, a control scheme based on a new adaptive DOB is proposed to suppress high-frequency wide-spectrum vibrations in HDD systems. To handle the time-varying characteristics of the center frequency and spectral peak width of the vibrations, a new lattice-form notch filter is introduced to design the Q filter in DOB such that the passband width of the Q filter can be adaptively tuned in the presence of different vibrations. Simulations on an open-source HDD benchmark show that the proposed algorithm can adaptively tune the passband width parameter which maximally attenuates the main spectral peak in the error signal with minimal performance sacrifice at other frequencies.

References

[1] X. Chen and M. Tomizuka. Unknown multiple narrow-band disturbance rejection in hard disk drives - an adaptive notch filter and perfect disturbance observer approach. In *proceedings of 2010 ASME Dynamic Systems and Control Conference*, pages 963–970, Cambridge, Massachusetts, USA., September 13-15 2010. ASME.

[2] X. Chen and M. Tomizuka. Inverse-based local loop shaping and iir-filter design for precision motion control. In *proceedings of 2013 IFAC Symposium on Mechatronic Systems*, pages 490–497, Zhejiang University, Hangzhou, China, September 10-12 2013. IFAC.

[3] Xu Chen and M. Tomizuka. A minimum parameter adaptive approach for rejecting multiple narrow-band disturbances with application to hard disk drives. *Control Systems Technology, IEEE Transactions on*, 20(2):408–415, March 2012.

[4] Xu Chen and Masayoshi Tomizuka. Selective model inversion and adaptive disturbance observer for time-varying vibration rejection on an active-suspension benchmark. *European Journal of Control*, 19(4):300–312, 2013.

[5] R. Ehrlich and D. Curran. Major hdd tmr sources and projected scaling with tpi. *Magnetics, IEEE Transactions on*, 35(2):885–891, Mar 1999.

[6] Lin Guo and Y.-J.D. Chen. Disk flutter and its impact on hdd servo performance. *Magnetics, IEEE Transactions on*, 37(2):866–870, Mar 2001.

[7] M. Hirata. Nss benchmark problem of hard disk drive system, 2007. http://mizugaki.iis.u-tokyo.ac.jp/nss/.

[8] Qing-Wei Jia. Disturbance rejection through disturbance observer with adaptive frequency estimation. *Magnetics, IEEE Transactions on*, 45(6):2675–2678, June 2009.

[9] Ioan Dore Landau, Aurelian Constantinescu, and Daniel Rey. Adaptive narrow band disturbance rejection applied to an active suspension-an internal model principle approach. *Automatica*, 41(4):563–574, 2005.

[10] J. Levin and P. Ioannou. Multirate adaptive notch filter with an adaptive bandwidth controller for disk drives. In *American Control Conference, 2008*, pages 4407–4412, June 2008.

[11] Arye Nehorai. A minimal parameter adaptive notch filter with constrained poles and zeros. *Acoustics, Speech and Signal Processing, IEEE Transactions on*, 33(4):983–996, Aug 1985.

[12] K. Ohnishi. A new servo method in mechatronics. *Transactions of Japanese Society of Electrical Engineering*, 107(D):83–86, 1987.

[13] P.A. Regalia. An improved lattice-based adaptive iir notch filter. *Signal Processing, IEEE Transactions on*, 39(9):2124–2128, Sep 1991.

[14] Abraham Castellanos Silva, Ioan Doré Landau, and Tudor-Bogdan Airimiţoaie. Direct adaptive rejection of unknown time-varying narrow band disturbances applied to a benchmark problem. *European Journal of Control*, 19(4):326 – 336, 2013.

[15] Liting Sun, Xu Chen, and Masayoshi Tomizuka. Adaptive suppression of high-frequency wide-spectrum vibrations with application to disk drive systems. In *2014 ASME Dynamic Systems and Control (DSC) Conference*, San Antonio, Texas, USA, October 2014.

[16] D. Vesset. Worldwide big data technology and services 2012-2015 forecast. March 2012.

[17] M.T. White, M. Tomizuka, and C. Smith. Improved track following in magnetic disk drives using a disturbance observer. *Mechatronics, IEEE/ASME Transactions on*, 5(1):3–11, Mar 2000.

[18] Qixing Zheng and M. Tomizuka. A disturbance observer approach to detecting and rejecting narrow-band disturbances in hard disk drives. In *Advanced Motion Control, 2008. AMC '08. 10th IEEE International Workshop on*, pages 254–259, March 2008.